21st European Workshop on White Dwarfs
Castanheira, Vanderbosch, Montgomery, eds.
July 23–27, 2018, Austin, Texas, USA

Revisiting the White Dwarf Luminosity Function from the Palomar-Green Survey

A. Bédard, P. Bergeron, and G. Fontaine

Université de Montréal, Montréal, Québec, Canada;
bedard@astro.umontreal.ca, bergeron@astro.umontreal.ca, fontaine@astro.umontreal.ca

Abstract

We present updated atmospheric parameters for all DA, DB, and DO white dwarfs in the complete sample of the Palomar-Green survey. In particular, we perform a spectroscopic analysis of the DO stars using our new set of non-LTE model atmosphere calculations. We then compute an improved luminosity function of the Palomar-Green sample, including the DO stars for the first time, which allows us to study the variations in the numbers of hydrogen- and helium-atmosphere white dwarfs along a large part of the cooling sequence. We demonstrate that the so-called float-up model successfully explains the spectral evolution of the majority of white dwarfs.

1 Introduction

As they evolve, white dwarf stars undergo major changes in their surface chemical composition, a phenomenon referred to as spectral evolution. The most striking manifestation of this process is the existence of the DB gap, a range in effective temperature ($45,000$ K $> T_{\rm eff} > 30,000$ K) where a significant deficiency of helium-atmosphere white dwarfs is observed. One possible explanation for this feature is offered by the so-called float-up model, first devised by Fontaine & Wesemael (1987), according to which most white dwarfs are the progeny of the hot helium-rich PG 1159 stars, but contain residual hydrogen thoroughly mixed (and thus hidden) in their helium envelope. As they cool down, the hydrogen gradually diffuses upward and accumulates at the surface, ultimately transforming all helium-dominated atmospheres into hydrogen-dominated atmospheres above 45,000 K. On the other hand, the reappearance of helium-rich white dwarfs below 30,000 K is thought to result from the onset of convection in the underlying helium envelope, which dilutes the hydrogen layer if the latter is thin enough. With the aim of exploring the float-up model, we revisit the white dwarf luminosity function of the Palomar-Green (PG) survey (Green et al., 1986), which allows us to study the variations in the numbers of DA and non-DA stars along the cooling sequence. To do so, we derive atmospheric parameters for all 348 DA, 47 DB and 12 DO white dwarfs in the complete PG sample through spectroscopy. Our analysis takes into account the latest theoretical developments (such as state-of-the-art Stark broadening profiles and 3D hydrodynamical corrections) and includes the DO stars for the first time, which constitute two notable improvements over previous studies of the PG luminosity function.

2 Atmospheric Parameters

The atmospheric parameters of the DA stars were taken from Gianninas et al. (2011) and corrected for 3D hydrodynamical effects following the prescription of Tremblay et al. (2013), while those of the DB stars were obtained using the model atmospheres, synthetic spectra and fitting procedure described in Rolland et al. (2018).

In order to perform a spectroscopic analysis of the 12 DO white dwarfs, we constructed a new grid of non-LTE model atmospheres and synthetic spectra with a pure helium composition using the codes TLUSTY and SYNSPEC (Hubeny & Lanz, 1995). These new models incorporate the He I line profiles of Beauchamp et al. (1997), which we implemented in both codes, and the He II line profiles of Schoening & Butler (1989). Our grid covers a range of $T_{\rm eff} = 40,000 - 150,000$ K and $\log g = 6.5 - 9.5$. We also calculated a similar grid of models including hydrogen since one of our DO stars (PG 1612+112) is actually a DOA star.

The spectroscopic observations were either secured at the Steward Observatory 2.3 m Bok telescope equipped with the Boller & Chivens spectrograph (7 objects), retrieved from the SDSS database (2 objects), or kindly provided to us by Klaus Werner (3 objects). In order to obtain the best-fitting atmospheric parameters,

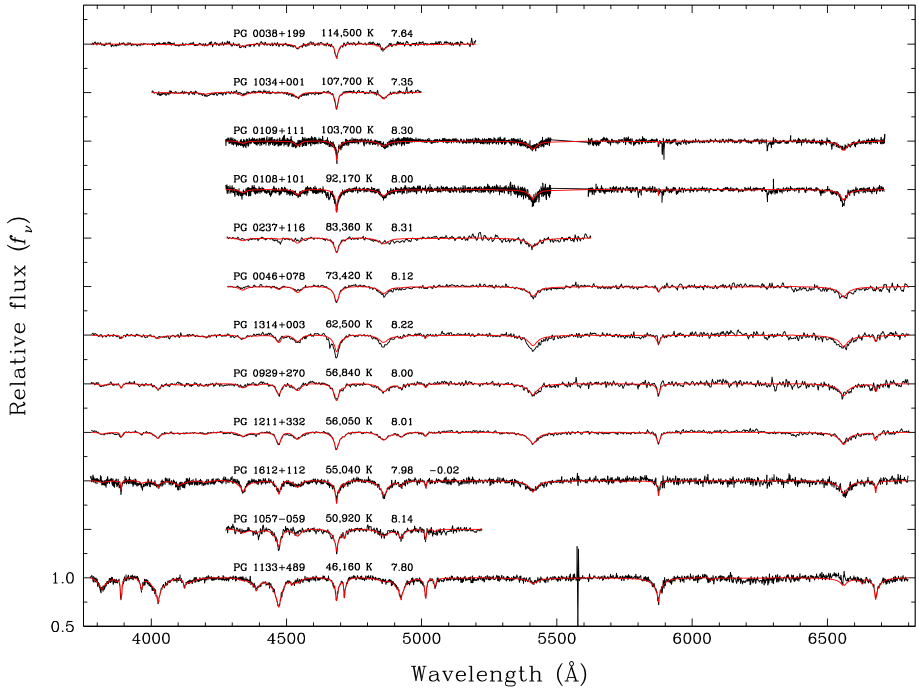

Figure 1: Best fits to the optical spectra of the DO white dwarfs, each offset by 0.5 for clarity. The observed and theoretical spectra are displayed as black and red lines, respectively. The atmospheric parameters are given in the figure.

the observed and model spectra were first normalized to a continuum set to unity, and the difference between these normalized spectra, defined as a χ^2 value, was then minimized using a nonlinear least-square method. The best fits are shown in Figure 1 in order of decreasing effective temperatures, together with the corresponding $T_{\rm eff}$ and $\log g$ values. For PG 1612+112, we also give the hydrogen abundance (by number), $\log {\rm H/He} = -0.02$, which is extremely high by DO standards.

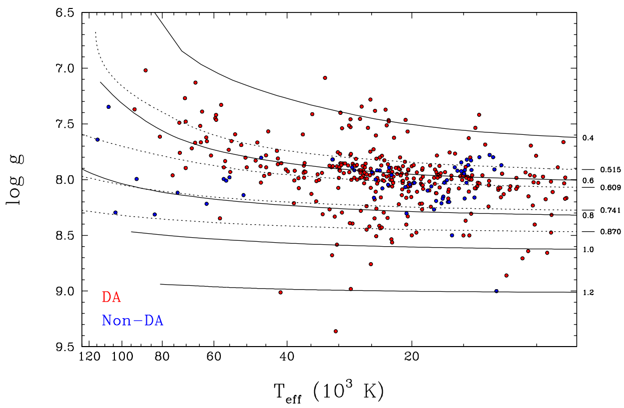

Figure 2: Surface gravities as a function of effective temperatures for all DA (red) and non-DA (blue) white dwarfs in our sample, together with H-rich (solid lines) and He-rich (dotted lines) evolutionary sequences (labeled by their mass, in solar masses) from Wood (1995) and Althaus et al. (2009), respectively.

We present in Figure 2 the $\log g - T_{\rm eff}$ diagram for all DA (red) and non-DA (blue) white dwarfs in our sample. For each object, evolutionary sequences were used to calculate the radius, mass and luminosity from the atmospheric parameters. Below 30,000 K, we relied on the carbon/oxygen-core models of Fontaine et al. (2001) with hydrogen envelopes of $M_{\rm H}/M_\star = 10^{-4}$ and 10^{-10} for DA and DB stars, respectively. Above 30,000 K, we employed the carbon-core models of Wood (1995) with hydrogen layers of $M_{\rm H}/M_\star = 10^{-4}$ for DA stars, while we made use of the carbon/oxygen-core, hydrogen-free models of Althaus et al. (2009) for DO stars. Figure 2 displays some of the evolutionary sequences (labeled by their mass, in solar masses), from Wood (1995) and Althaus et al. (2009) as solid and dotted lines, respectively.

3 Mass Distribution

Figure 3 shows the mass distribution as a function of effective temperature for all DA (red) and non-DA (blue) stars in our sample. Overplotted are theoretical isochrones representative of hydrogen-rich white dwarfs (labeled by their value of $\log \tau$, where τ is the cooling age in years) obtained from the evolutionary models of Wood (1995) for $\log \tau < 8$ and Fontaine et al. (2001) for $\log \tau \geq 8$. The mass distribution is centered around $\sim$0.6 $M_\odot$ throughout the entire temperature

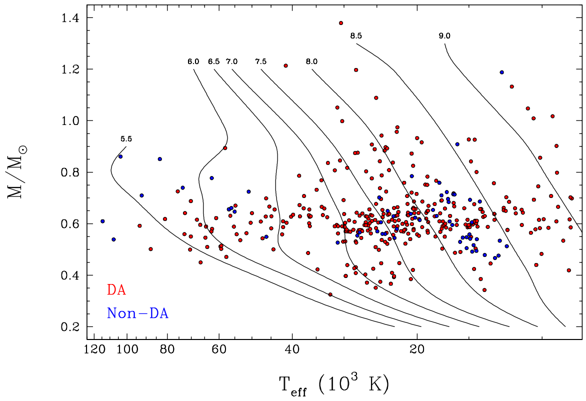

Figure 3: Stellar masses as a function of effective temperatures for all DA (red) and non-DA (blue) white dwarfs in our sample, together with H-rich theoretical isochrones (labeled by their value of $\log\tau$, where τ is the cooling age in years) from Wood (1995) for $\log\tau < 8$ and Fontaine et al. (2001) for $\log\tau \geq 8$.

range. Furthermore, the paucity of helium-rich white dwarfs in the range $45,000$ K $> T_{\rm eff} > 30,000$ K is obvious. Note that our sample does not include DC stars, into which DB stars evolve at $T_{\rm eff} < 12,000$ K, hence the apparent lack of non-DA white dwarfs at the cool end.

Figure 4 displays the cumulative mass distribution of our whole sample (black), as well as the DA (red) and non-DA (blue) components. The mean value and standard deviation of each distribution are given in the panel. While the DA histogram exhibits a sharp central peak but also contains a low-mass and a high-mass tails, the non-DA histogram is rather extended but contains very few low-mass and high-mass objects. Despite these differences, the mean values of the DA and non-DA mass distributions are in excellent agreement with each other and are comparable to other values reported in the literature.

4 Luminosity Function

Our improved luminosity function, which gives the number of white dwarfs per cubic parsec and per absolute bolometric magnitude, was computed employing the so-called $1/V_{\rm max}$ method (Liebert et al., 2005) and is presented in Figure 5 (black). The DA (red) and non-DA (blue) luminosity functions are displayed as well. As a reference, we also show the effective temperature scale corresponding to a 0.6 $M_\odot$ helium-rich white dwarf. At the hot end ($M_{\rm bol} < 2$), DA and DO stars make a similar contribution to the luminosity function. Then, the relative contribution of non-DA white dwarfs decreases in the range $2 < M_{\rm bol} < 5$, and essentially vanishes in the range $5 < M_{\rm bol} < 7$, which corresponds to the DB gap. DB white dwarfs appear in the range $7 < M_{\rm bol} < 11$, although their contribution becomes important only for $M_{\rm bol} > 9$. At the cool end ($M_{\rm bol} > 11$), our luminosity function is incomplete since DB stars turn into DC stars, which were excluded from our analysis.

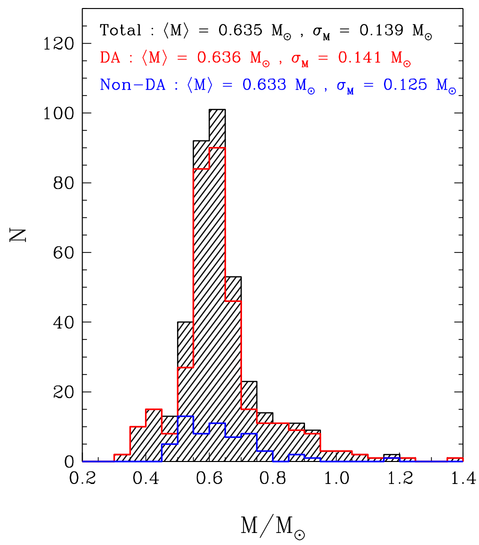

Figure 4: Cumulative mass distribution of our whole sample (black), and of the DA (red) and non-DA (blue) white dwarfs. The mean value and standard deviation of each distribution are given in the figure.

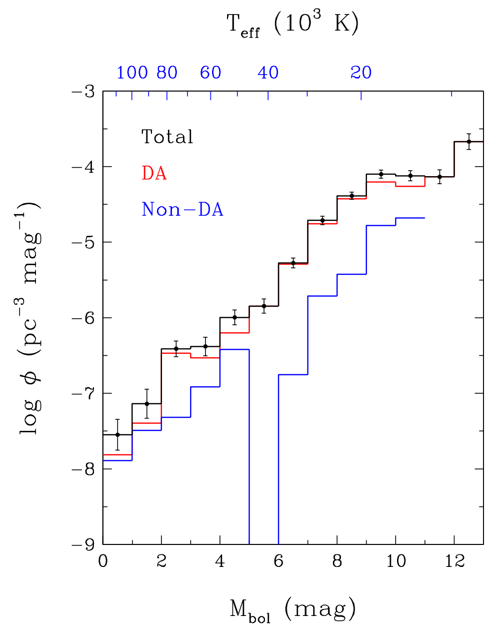

Figure 5: Luminosity function of our whole sample (black), and of the DA (red) and non-DA (blue) white dwarfs. The effective temperature scale of a 0.6 $M_\odot$ helium-rich white dwarf is shown at the top of the plot.

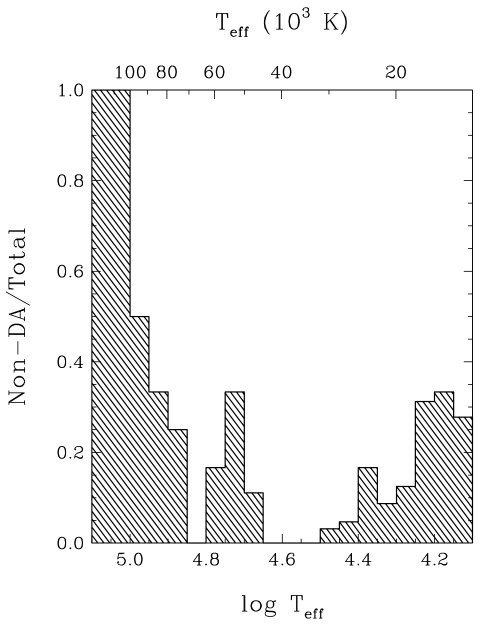

Figure 6: Fraction of non-DA white dwarfs in our sample as a function of effective temperature.

A more intuitive approach for studying the spectral evolution of white dwarfs is to simply consider the fraction of non-DA stars as a function of effective temperature, which is presented in Figure 6. We notice that the fraction of non-DA white dwarfs gradually decreases from 1 at $T_{\rm eff} = 100,000$ K to 0 at $T_{\rm eff} = 45,000$ K. Note that the empty bin near $T_{\rm eff} = 70,000$ K stems from small-number statistics — our sample comprises only 26 stars hotter than 60,000 K — and is thus not meaningful. However, the complete absence of non-DA white dwarfs in the range $45,000$ K $> T_{\rm eff} > 30,000$ K is undoubtedly significant, since 45 objects are found there, yet none of them harbor a helium-dominated atmosphere. Then, on the other end of the gap, non-DA stars reappear at the ∼10% level below $T_{\rm eff} = 30,000$ K, and at the ∼30% level below $T_{\rm eff} = 20,000$ K.

5 Discussion and Conclusion

Our results can be interpreted as strong evidence in favor of the float-up model. Indeed, the gradual decrease in the fraction of helium-atmosphere white dwarfs at high temperature can be associated with the transformation of DO stars into DA stars as a hydrogen layer is being built up from the upward diffusion of hydrogen. Moreover, even though DB stars appear in small numbers at 30,000 K, the bulk of them emerge at 20,000 K rather than 30,000 K. This is consistent with the idea that the convective helium envelope dilutes the thin hydrogen layer, since the helium convection zone becomes important below ∼20,000 K (Rolland et al., 2018). We also note that our value of ∼30% for the fraction of DB stars is somewhat higher than the canonical value of ∼20%.

However, this is not the full story. We know, thanks to the SDSS, that the DB gap is rather a DB deficiency since it actually contains a few helium-rich objects (Eisenstein et al., 2006). This indicates that there must be a second evolutionary channel involving a small fraction of white dwarfs that are born completely devoid of hydrogen and hence retain a helium-dominated atmosphere throughout their evolution. In addition, several very hot DA stars have been found over the years, implying that there exists a third evolutionary channel in which white dwarfs do not descend from PG 1159 stars and always remain hydrogen-rich. Nevertheless, the revised luminosity function of the PG survey demonstrates that the float-up model most certainly applies to a significant fraction of the white dwarf population and provides a viable explanation for the existence of the DB gap.

References

Althaus L. G., Panei J. A., Miller Bertolami M. M., García-Berro E., Córsico A. H., Romero A. D., Kepler S. O., Rohrmann R. D., 2009, ApJ, 704, 1605

Beauchamp A., Wesemael F., Bergeron P., 1997, ApJS, 108, 559

Eisenstein D. J., et al., 2006, AJ, 132, 676

Fontaine G., Wesemael F., 1987, in Philip A. G. D., Hayes D. S., Liebert J. W., eds, IAU Colloq. 95: Second Conference on Faint Blue Stars. pp 319–326

Fontaine G., Brassard P., Bergeron P., 2001, PASP, 113, 409

Gianninas A., Bergeron P., Ruiz M. T., 2011, ApJ, 743, 138

Green R. F., Schmidt M., Liebert J., 1986, ApJS, 61, 305

Hubeny I., Lanz T., 1995, ApJ, 439, 875

Liebert J., Bergeron P., Holberg J. B., 2005, ApJS, 156, 47

Rolland B., Bergeron P., Fontaine G., 2018, ApJ, 857, 56

Schoening T., Butler K., 1989, A&AS, 78, 51

Tremblay P.-E., Ludwig H.-G., Steffen M., Freytag B., 2013, A&A, 559, A104

Wood M. A., 1995, in Koester D., Werner K., eds, Lecture Notes in Physics, Berlin Springer Verlag Vol. 443, White Dwarfs. p. 41, doi:10.1007/3-540-59157-5_171